行政院國家科學委員會專題研究計畫成果報告
新中橫公路沿線地質環境之特性（III）

The characteristics of geological environment along the New East-West cross highway (III)

計畫編號：NSC 89-2116-M-002-020

計畫主持人：陳宏宇　　計畫參與人員：林世榮、王瑞斌、游家敏

執行機構及單位名稱：台灣大學地質科學研究所

Abstract

By an onsite investigation, the largest debris flow in Taiwan's history is analyzed in this paper. A heavy rainfall of 1748 mm/day occurred during typhoon Herb in the Hoser area at the end of July 1996. Aerial photo assessment and observations of geological and geomorphological features have contributed to our understanding of this massive destruction. Mechanisms of the hazardous debris flow are explored and discussed.

Data revealed that the rock discontinuities were a major factor in the voluminous loose materials in the debris flows. The heavy and rapid rainfall instantly transported massive amounts of debris flow materials into the center and then quickly funneled them to the lower parts of gullies. The heavy slurry became an effective cutting device to erode the sidewalls and move large quantities of the debris materials to the end of the gullies.

Key words: hazard, debris flow, discontinuity, geomorphology

中文摘要

本文以現場調查之觀點來分析台灣史上最大的土石流災害。1996**年**7**月底，賀伯颱風給和社地區帶來了**1748mm**的日降雨量。從航照圖的分析以及其他地質、地貌表徵的調查工作有助於我們收集大量的資料對於破壞現象的了解，而土石流災害的機制也一併在現地調查工作中討論。**

從現地調查的資料中顯示，岩石不連續面的崩解，突然使得溝谷兩旁之地質材料堆積於溝谷中，是造成本次災害的主因。而大量及迅速的降雨，將這些堆積於溝谷中的地質材料不停的運往下游。這些瞬間形成的土石流不僅往下流動，也一面對溝谷兩側的谷壁產生淘挖、沖蝕的現象，並同時將兩側崩坍之土石匯聚於溝谷中，一併往下面流動至溝谷底部。

關鍵詞：災害、土石流、不連續面、地貌

Introduction

Typhoon Herb dropped a great volume of precipitation at the rate of 1748mm/day in the Hoser area at the end of July 1996. An enormous flood re-deposited huge quantities of material from devastating liquid flows without warning. This violent storm resulted in serious damage and loss of property totaling around 600 million US dollars in central Taiwan.

Hoser is in the southern part of Nantou county in central Taiwan (Fig. 1), along the western part of the Hoser River. It makes up a total area of around 10 Km^2. No.1 and No.3 gullies were selected for the present investigation. The elevation of the study area ranges from 820 meters to 1150 meters above sealevel. It is a rugged hilly area having slopes from 15^o to 45^o.

Typhoon Herb brought about flash flood events and huge massive material movements. Debris flows transported erosive materials down to the bottom of the gullies. Disintegrated materials came out from the upper to the middle parts of the gullies just behind the villages (Chen and others 1999; Chen 2000).

Conditions for debris flows include specific local geomorphology, geological characteristics, quantity of geomaterials and degree of saturation by groundwater (Johnson and Rodine 1984; VanDine 1985; Baldwin and others 1987; Takahashi 1991).

Geomorphological studies of this area have been based on aerial photography from 1980 to 1996. Also detailed onsite observations in terms of geology and geomorphology, provide a better understanding of the origin of the debris flows in the study area. Topographical changes in the gully beds and mountain slopes are herein compared to aerial photography before and after the debris flows. Discontinuities of rocks and slope stability are thoroughly investigated and analyzed in the present study.

Geological condition

The rock types along the west part of the Hoser River consist of massive shale, sandy shale and fine interbeds of sandstone and shale. They belong to the Hoser Formation of the Miocene age (Ho 1986). It is easy to find some flexural slip folds and relative displacements in the rock formation. Cementation is not very good in various rocks and appears highly fractured.

The axis of the Hoser anticline passes through the center of the study area in a north-south direction. Different sets of discontinuities have intervals from 10cm to 1 meter. The strike of the bedding in the western part of the study area ranges from N31^{o}E to N42^{o}E and dip from 60^{o} to 68^{o} towards the northwest. The three sets of joints are: (A) N30^{o}E with a southerly dip of 85^{o}; (B) N35^{o}W with a northerly dip of 40^{o}; and (C) N70^{o}W with a southerly dip of 50^{o}. Calcite and quartz commonly fill the discontinuities. The densely distributed discontinuities cut up massive rocks and form huge volumes of fractured rocks and debris on various slopes waiting for movement.

Aerial photography

Photographs in five periods, 1980, 1985, 1988, 1993 and 1996 were used to compare the consecutive changes of erosive forces in the Hoser area. The overall geomorphology of the study area can be readily traced by these aerial photographs. The existing slope collapses on the ground surface and the gully channels can also be quickly traced (Rib and Liang 1978; Shlemon and others 1987).

(1) 1980

The mouth of No.1 gully shows little sign of deposition or movement of material. Vegetation and trees were naturally distributed in their evidently original state on the slope. The uphill slope areas of the gully show no deposits or collapses on both sides. On the western part of the Hoser River, some images are nearly too small to distinguish in the photos. No.1 gully and the other watershed divide are very clear. The lateral lobes in the study area have not yet been produced. A delta fan at the mouth of the gully was obviously formed long ago. Many farm fields have already been produced on the slope. No.3 gully also shows no evidence of deposited material or collapsed conditions.

(2) 1985

There are no obvious changes in their topography after 5 years at No.1 and No.3 gullies.

(3) 1988

The area in the middle parts of No.1 and No.3 gullies have changed slightly in their topography after 8 years. The farm areas around both gullies have obviously increased in size and number.

(4) 1993

The vegetation changed slightly uphill of No.1 and No.3 gullies. The shape of the gullies was only altered a little. Neither was there was evidence of erosion or material movement in the gully. The farm areas near the gullies have multiplied in number and area, at the cost of native plants increasingly removed—increasing the risk of erosion.

(5) 1996

After typhoon Herb, the morphology changed fundamentally. The original vegetation was removed by cutting and by erosion of the chaotic debris flow materials. The gully channels became wider than in 1993. The gullies now obviously show deposited materials and huge material movement. The original areas of No.1 and No.3 have had large collapses on both sides of their gullies. Big lobes have formed on the collapsed areas. Their mouths have received masses of deposited geomaterials, forming new alluvial deltas. The lengths, widths and depths of the deposits in the gullies have increased dramatically.

The various photographs from the 5 different periods demonstrate that the gully shapes and widths changed little before the debris flow hazard at the end of the 15 years.

A very complex network was formed by the tributary streams on both sides of the Hoser River over this 15-year period. The morphology of No. 1 and No.3 gullies also totally changed after typhoon Herb. Figure 8 clearly shows that the widths of both gullies appear to be 5 times what they were in 1993.

The watershed areas on the mountain sides above both gullies experienced a large number of collapses - particularly at the heads of the gullies. Steep scars on both sides of both gullies have become evident and developed over their whole distance. The resulted widened valleys were clearly visible in the aerial photographs.

The mouths of both gullies have widened, and their delta fans have been much enlarged. Their small lateral lobes have been eroded and combined with the main (No.1 & No.3) gullies. Many trees were swept away from their original locations. Villages along the Hoser River were wiped out in the major disaster.

Geomorphology

The components of debris flows are mainly of 3 different parts. The main triggering debris flow material comes from the area of origin. The second major component - the flow area - is composed of the moving material from the upper part combining with water in its flow to the bottom of the gully. The terminal resting location of formerly moving geomaterial forms the depositional area (Fyleming and others 1989), which normally takes a delta fan shape. Deposited geomaterials are typically described as coarse, poorly sorted, unstratified and unconsolidated (Costa and Jarrett 1981; Johnson and Rodine 1984; Shlemon and others 1987).

Debris flows occur as slope deposits are set in motion by massive runoff. The deposition of levees may begin at 15°. The slope gradient on the deposited area tends to be gentle. Upper gully geomaterial deposits must reach a sufficient thickness to support the initiation of a debris flow Campbell 1974; Baldwin and others 1987). Sufficient precipitation is all that is necessary to set off the triggering mechanisms of a devastating debris flow (Eyles 1979; Nielsen 1984).

Understanding the respective contributions of these three areas of the debris flow can help in the articulation and comprehension of the hazardous area under study. The accumulative deposits on the river bank have gradually occurred as demonstrated by aerial photographs spanning the last 15 years in the Hoser River. Each debris flow formed a lobe as it filled a concave area which had been left by the preceding lobes.

In the site observation, the cohesion of the geomaterial appears to be quite weak to nonexistent. The geomaterial in an initial flow and after-flow condition tends to be very difficult to differentiate at the same site section. The angular and rounded form of the rock fragments and boulders provides a critical clue about whether the material is part of an initial flow or an after-flow. It could be determined by field observation whether the rock fragments are historically rounded or recently angular. These observations show that the original geomaterials are freshly broken " in-situ " or have already been transported for a long distance in the gully from higher locations.

Site condition

The area of origin forms a hollow topography on the uphill of No.1 and No.3 gullies, and was formed by the drag fold of a syncline structure. The diameter of this hollow is 23 meters and contains the collapsed material from both sides of the gullies. The erosion cuts an average of 1 meter to 5 meters deep on the channel of both gullies. The thickness on the deposited area is around 1.5 meters.

The 34 profiles, made every 25 meters, were used for section analysis at No.1 gully. This method enabled a better comprehension of the changes of the topography before and after the collapse along the gully . The gully formed a V-shape before the hazard at elevations of 1023 to 970 meters. The slope gradient before collapse was 18^o .

The gully containing the debris deposits forms a U-shape after the collapse. The slope gradient now averages 15^o. The results of the comparison on the topography demonstrate that the gully was eroded downward and outward to both sides. This also changed the cross-section from a "V" to more of a "U". The erosion cut an average of 6 meters deeper into the topography. The deepest cutting area was about 11 meters.

Some parts of the flow section still appear in an eroded condition and others in a deposited one between the elevations of 970 to 868 meters. The slope gradient changed from 20^o before the hazard to 17^o after. These conditions signal a potential flow section in a future deluge.

The depositional sections of the gully between the elevation 868 to 820 meters formed a "U" shape before the debris flow. This "U" shape was retained after the debris flow. The slope gradient is very gentle from 11^o to 9^o. The thickness of the depositional area was now about 11 meters. The maximum thickness grew to 17 meters.

The 71 profiles, taken from every 25 meters, were used for section analysis at No.3 gully . The gully formed a V-shape before the hazard at elevations of 1,152 to 1,002 meters. The slope gradient before the hazard was 19^o The gully forming the debris deposit has a U-shape in its cross-section after the collapse. The slope gradient now averages 15^o. Comparison of the topography of No. 3 gully reveals that the gully was eroded downward and outward to both sides. The erosion cut an average of 6 meters. The deepest cut area was now about 9 meters.

The flow section still appears in an eroded or deposited state between the elevations of 1,002 to 945 meters. The slope gradient changed from 13° before to 11° after the hazard. This flow section contains serious downward cutting. However, all parts of the gully section under elevation 945 meters take on depositional features. This local region is now defined as the depositional section. The erosional cutting here is about 6 meters.

The lower sections between the elevation of 945 to 891 meters took a "U" shape before the debris flow. This "U" shape has been retained after the debris flow. The slope gradient becomes very gentle from 10^o to 8^o. The thickness is around 8 meters. The maximum thickness here is about 15 meters.

The volume of deposited geomaterial from the debris flow on the channel of No. 1

gully was about 490350 m^3. A total of 48020 m^3 was deposited in the middle part of the gully, and another volume of about 442330 m^3 in the delta fan which is between the mouth of the gully and the Hoser River. In No.3 gully, the volume of deposits was about 985572 m^3. A total of 221547 m^3 was deposited in the middle part of the gully, and another volume of around 764025 m^3 in the delta fan. It is also located between the mouth of the gully and the Hoser River.

Close observation of the debris flow can demonstrate whether the origination of geomaterial sources are from freshly broken in-situ materials or from other older materials. Some caotic materials have already been transported for a long distance in the gully from higher locations. Mixture of the deposited material includes rock fragments and fine particles. The size of big boulders is about 1 to 4 meters. Their shapes appear subangular to angular and its lithology is fresh. The gully beds are normally empty of water. The slope gradient averages from around 30^o to 60^o.

Geomaterial properties

Geomaterials of the debris flow in the gully used in the model test was reconstituted with the field material. This was done in the laboratory experiments by using the "modified weight replacement method" with scaled down particles of maximum grain sizes of 1.5 in. (38.1mm), 1.0 in. (25.4 mm), and 0.5 in (12.7 mm) each. The main point of this method is to insure that the geomaterials have similar unit weight and porosity as those in-situ.

Su (1998) dug out 3 and 5 pits in 1 m x 1 m x 1m in both study areas. He took in-situ samples for physical properties tests from upper, middle and lower parts of each pits in the depositional area. The soil classification followed the unified soil classification system. These results demonstrated that each deposit on the individual study areas had similar physical properties (Table 1). To determine shear strengths of the gully sides, a direct shear test of the multistage method was used to test the geomaterials from the various discontinuities on both sides of the gully (Chen and others 1995). The experimental test on discontinuities included the geomaterials on schistosity, bedding and joints. In order to simulate the in-situ conditions, a large direct shear box of 30cm x 30cm x 15.3cm was used.

The geomaterial samples were taken for classification from the three different parts. In general, it has been found that the geological characteristics of the gully, and the mechanical behaviour of the geomaterials, are factors that affect the debris flow.

All samples taken from the test pits in No.1 gully, have no intrinsic cohesion and the friction angle ranging from 34^o to 36^o. But under the saturated condition, the friction angle ranges from 30^o to 31^o. In No.3 gully, it ranges from 34^o to 36^o, and under the saturated condition, from 29^o to 31^o.

In No.1 gully, the shear strength of the discontinuities plane was 29^o - 41^o under the dry condition, and 25^o - 33^o under the saturated state. In No.3 gully, it is 32^o - 38^o under the dry condition, and 27^o - 34^o under the saturated state. These discontinuities on the exposed gully sides form a potential wedge model. Table 2 shows the measured shear strengths on the contact plane of the discontinuities (Su 1998).

Stability condition

Stability analyses in this paper were conducted to understand potential behaviours of slopes on both sides of the gully. The analytical methods include discontinuities analyses and safety factor calculation. The stability analysis makes use of plane failure and wedge failure methods. The basic results on a potentially unstable slope are determined from a stereonet analysis.

The quantitative determination of the stability of a slope using any of the accepted methods should be based on a knowledge of the geological structure of the area and the geomorphological history of the land use (Graham 1984; Bromhead 1986). The safety factor is normally considered to represent the average reserve ability of the profile to resist the gravity forces and other external forces which act on the geomaterial mass of the slope.

Safety factor calculation

Both potentially unstable models have quantified safety factors (Hoek and Bray 1981). The dip slope formula is as follows:

$$F = \frac{c \times A + \left(W \cos\psi_\rho - U - V \sin\psi_\rho\right) \times \tan\phi}{W \sin\psi_\rho + V \cos\psi_\rho}$$

c: Cohesion, kN/m^2
ψ_ρ: Failure angle, degree
A: Length of slip surface, m
W: Weight of failure mass, t/m
U: Uplift force, t/m
V: Lateral water pressure, t/m
ϕ: Friction angle, degree

The wedge slope formula is:

$$F = \frac{(R_a + R_b)\tan\phi}{W \sin\varphi_i} = \frac{\sin\beta \times \tan\phi}{\sin\frac{1}{2}\xi \times \tan\varphi_i}$$

R_a, R_b: Normal stress on Mass A and Mass B
ξ: Intersected angle on Mass A and Mass B
ϕ: Friction angle
φ_i: Dip angle of intersection line on two discontinuities
β: Tilt angle of wedge

The present stability analysis includes the gully deposition besides both sides of the gully slope. For this, the infinite slope method is used. Its basic equation is given as follows:

$$F_s = \frac{\gamma_{sat} - \gamma_\omega}{\gamma_{sat}} \cdot \frac{\tan\phi}{\tan\theta}$$

γ_{sat}: Saturated unit weight
γ_w: Water unit weight
ϕ: Friction angle
θ: Failure angle

The above parameters of shear strength were taken from the laboratory tests and used to analyze the critical conditions for initiating a debris flow in the study areas.

Discontinuities analysis

The discontinuities analysis is a semiquantitative set of parameters and implications for the rock slope on both sides of gully. The geological attitude was measured by in-situ investigation and plotted in a stereonet. They include discontinuities of bedding, joints and diverse slope surfaces (Selby 1987; Priest 1992). They comprise various geometric shapes and set up the possibility of various potential failure models. These geometric types reveal themselves as potential failure models and clearly show a tendency for instability or even collapse of the slope.

Stability results on outcrop

Figure 2 displays the possible directions of block displacement such as the dip slope and wedge slope models on No.1 and No.3 gullies. The shadow area shows the potentially unstable slopes.

The safety factor of the outcrop at marks 1-2, 1-3 and 1-4 on both sides of No. 1 gully displays a potentially unstable state in a saturated condition. The failure model includes plane, wedge and topple failures. This result indicates a good stability under the normal dry condition. When these slopes are saturated, however, the safety factor will fall below 1.0 (Table 3), and the slope will fail.

The safety factor of the outcrop at marks 3-2, 3-4 and 3-5 on both sides of No.3

gully displays a potentially unstable state in the saturated condition. The failure model also includes plane, wedge and topple failure as well. This result is the same as in the former case.

Stability results on gully deposits

Under the normal dry condition of No.1 gully, the safety factors (Fs) are 1.13, and 1.08. This means that the deposits in the valley are normally in a stable state. In the fully saturated situation, the safety factors fall to 0.96 and 0.92, respectively (Table 4). These materials deposited in the gully floor would then be in a highly unstable state.

Under the normal dry condition of No. 3 gully, the safety factors (Fs) are 1.17, and 1.11. This means that the deposits in the valley are normally in a stable state. In the fully saturated situation, the safety factors fall to 0.96 and 0.90, respectively. These materials deposited in the gully floor would then be in a highly unstable state.

Discussions

This paper describes the geometry of debris flow sources and provides a better understanding of these sources developed in the gullies of the study area. However, regardless of the length of time of this accumulation, cohesion of the particles deposited in this manner appears to be quite weak to nonexistent.

The debris flow resulted from mixing of rock fragments, fine fractions and water moves down a gully with slope angles ranging from about 15^{o} to 25^{o}. Some experimental results demonstrated that the precipitation would increase the water content, produce pore water pressure and decrease the shear strength of the geomaterial (Sidle and Swanston 1982). Therefore, these deposits become, in effect, "loaded cannon" waiting for precipitation to trigger the debris flow and send a deluge rushing down the river bed, engulfing all in their path. Gully gradients of the origination, flow and deposited areas are a result of the confineability of the stream or the lack/presence of confinement of the stream and the ratio of the debris material to water (Wu and Swanston 1980).

Historically, relatively little debris flow material accumulated over a long time period of at least 15 years as verified by aerial photographs spanning the above period of study. The deposited rock fragments have a nearly equal axial ratio in their longitudial and horizontal directions. Their shapes appeared subrounded to rounded, and their morphology remains rough. The topography of the gully is continually changing, but its destruction potential remains enormous.

Conclusions

The topography of the area is outlined, and the necessity to study the debris flow hazards is urged. Prediction can be vital. Discontinuities can be a major factor in forming the accumulated deposits in the gully. The accumulated deposits are the main source of the debris flow once the disaster is triggered.

To study the development of a debris flow, the aerial photography is deemed essential. Based on the field investigation and laboratory tests, a debris flow is triggered and moved by a high intensity rainfall. The material is produced and supplied from both sides of the gully.

References

BALDWIN II JE, DONLEY HF, HOWARD TR (1987) On debris flow/avalanche mitigation and control, San Francisco Bay area, California, *Geol Soc America*, Reviews in Engng Geology II, Pp.223-236.

BROMHEAD EN (1986) The stability of slope, *Surrey University Press*, New York, 373p.

CAMPBELL RH (1974) Debris flow originating from soil slips during rainstorms in southern California, *Q J Engng Geo*, l 7, Pp.339-349.

CHEN H (2000) The geomorphological comparison of two debris flow and their triggering mechanisms, *Bull Engng Geology Environment*, 58 (4), Pp.297-308.

CHEN RH, LIN ML, CHEN H (1995) Mechanism of initiation of debris flow, In: *Cheng FY, Shew MS (eds) Urban Disaster Mitigation, Oxford, Elesevier Science*, Pp.231-243.

CHEN H, CHEN RH, LIN ML (1999) Initiation of the Tungmen Debris Flow, Eastern Taiwan, *J. Environ Engng Geoscience*, V (4), Pp.459-473.

COSTA JE, JARRET RD (1981) Debris flows in small mountain stream channels of Colorado and their hydrologic implications, *Bull Assoc Engng Geologists*, 18, Pp.309-322.

EYLES RJ (1979) Slip-triggering rainfalls in Wellington city, New Zealand, *New Zealand J Sci*, 22 (2), Pp.117-122.

FYLEMING RW, ELLEN SD, ALGU MA (1989), Transformation of dilative and contractive landslide debris into debris flows-an example from Martin County, California. *Engng Geology*, 27, Pp.201-223.

GRAHAM J (1984) Methods of stability analysis. In: Brusden D, Prior DB (eds) *Slope instability*, John Wiley Sons, New York, Pp.171-215.

HO CS (1986) An introduction to the geology of Taiwan: Explanatory of the geologic map of Taiwan. The Ministry of Economic Affairs, Republic of China, 153p.

HOEK E, BRAY J (1981) Rock slope engineering, *The Institution of Mining and Metallurgy*, London, Pp150-198.

JOHNSON AM, RODINE JR (1984) Debris flow. In: Brunsden D, Prior D (eds) *Slope instability*, John Wiley Sons, New York, Pp.257-361.

NIELSEN HP (1984) Geology, rainfall and groundwater associated with several debris flows in Santa Cruz County, California. MSc thesis, University of California at Santa Cruz, 104 p.

PRIEST SD (1992) *Discontinuity analysis for rock engineering*, Chapman Hall, London, 420 p.

RIB HT, LIANG T (1978) Recognition and identification. In: Schuster RL, Krizek RJ (eds) Landslides analysis and control, Special report, 176, Pp.34-80.

SELBY MJ (1987) Rock slopes. In: Anderson MG, Richards KS (eds) *Slope stability*, John Wiely Sons, New York, Pp.475-504.

SHLEMON RJ, WRIGHT RH, MONTGOMERY DR (1987) Anatomy of a debris flow, Pacifica, California. Geol Soc America, Reviews in Engng Geology, VII, Pp.181-199.

SIDLE RC, SWANSTON DN (1982) Analysis of a small debris flow in coastal Alaska. Canadian Geotech J, 19 (2), Pp.167-174.

TAKAHASHI T (1991) *Debris Flow,* IAHR Balkema, 165p.

VANDINE DF (1985) Debris flow and debris torrents in the Southern Canadian Cordillera, Canada Geotech J, 22, Pp.44-62.

WU TH, SWANSTON DN (1980) Risk of landslides in shallow soils and its relation to cutting in southeastern Alaska, *Forest Sci*, 26 (3**),** Pp.495-510.

Table 1 Test result of physical properties of deposits in No.1 and No. 3 gullies of Hoser area

Area	Pit No.	Content of gravel (>2cm), (%)	Water content, (%)	Unit weight, (t/m^3)	Void ratio, (%)	Degree of saturation, (%)
Hoser	P_1-1	89.4	3.7	2.11	0.45	32.1
	P_1-2	81.8	4.3	1.79	0.51	28.5
	P_1-3	77.7	5.7	1.85	0.48	30.4
	P_3-1	78.5	4.6	1.94	0.46	29.7
	P_3-2	72.7	3.8	2.05	0.41	28.1
	P_3-3	75.1	3.4	1.83	0.43	25.4

* P_1: Pits in No. 1 gulley. P_3: Pits in No. 3 gulley.

Table 2 Results of the shear strength of discontinuity in No. 1 and No. 3 gullies of Hoser area

Area	Discontinuity	Sample condition	Sample no.	Friction angle, °	Remark
Hoser	Bedding plane	air dry	12Hbd	32.0	No.1 gully
			32Hbd	29.0	No.3 gully
		Saturated	12Hbw	31.5	No.1 gully
			32Hbw	24.0	No.3 gully
	Joint plane	air dry	13Hjd 14Hjd	39.0 41.0	No.1 gully
			32Hjd 33Hjd	34.0 38.0	No.3 gully
		Saturated	13Hjw 14Hjw	33.0 32.5	No.1 gully
			32Hjw 33Hjw	28.0 34.0	No.3 gully

※ (No intrinsic cohesion appeared in discontinuity)
H: Hoser, j: joint plane, b: bedding plane,
d: air dry, w: saturated

Table 3 The results of safety factor on the outcrope of both sides in No. 1 and No. 3 gullies.

Gully	Sample No.	θ (°)	ψ (°)	F	Remark
No.1	112D	48	32.0	1.11	Plane failure
	112S	48	31.5	0.97	
	122D	46	32.0	1.64	Stable
	122S	46	32.5	1.24	
	133D	61	39.0	1.05	Wedge failure
	133S	61	33.0	0.80	
	144D	72	41.0	1.14	
	144S	72	32.5	0.70	
No.3	322D	40	29.0	1.20	Plane failure
	322S	40	24.0	0.97	
	323D	36	34.0	1.32	Wedge failure
	323S	36	28.0	0.97	
	344D	49	31.5	1.38	
	344S	49	27.0	0.92	
	355D	78	34.5	1.19	
	355S	78	32.0	0.90	

※ D: dry condition, S: saturated condition,
θ : slope grade of gully, ψ: friction angle, F: safety factor

Table 4 The results of safety factor on the accumulated deposition of No. 1 and No. 3 gullies.

Gully	Sample No.	θ (°)	ψ (°)	F
No. 1	105D	18.1	35.6	1.13
	138D	18.1	34.4	1.08
	105S	18.1	31.3	0.96
	138S	18.1	30.2	0.92
No. 3	305D	18.5	36.2	1.17
	338D	18.5	34.7	1.11
	305S	18.5	31.1	0.96
	335S	18.5	29.4	0.90

※ D: dry condition, S: saturated condition,
θ : slope grade of gully, ψ: friction angle, F: safety factor

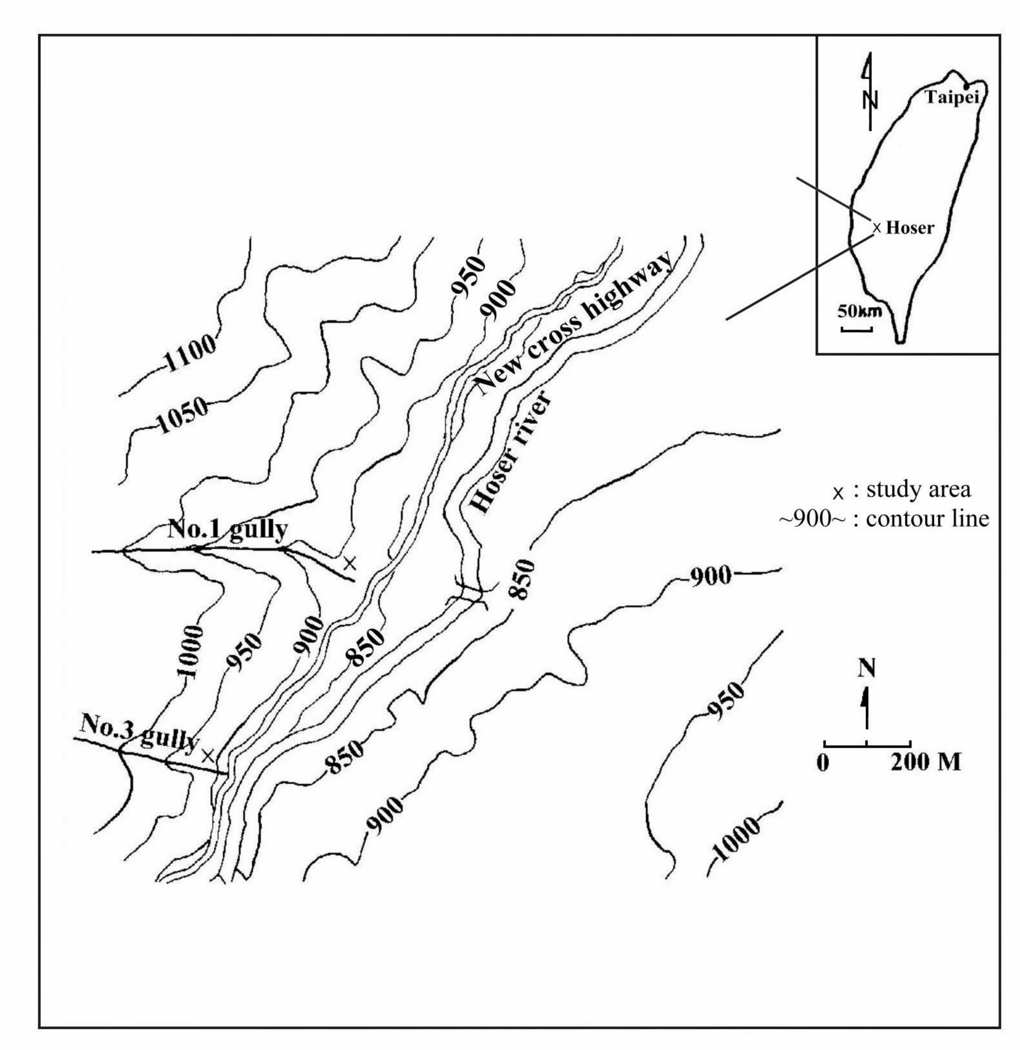

Fig. 1 The study area, Hoser is located in the middle part of Taiwan

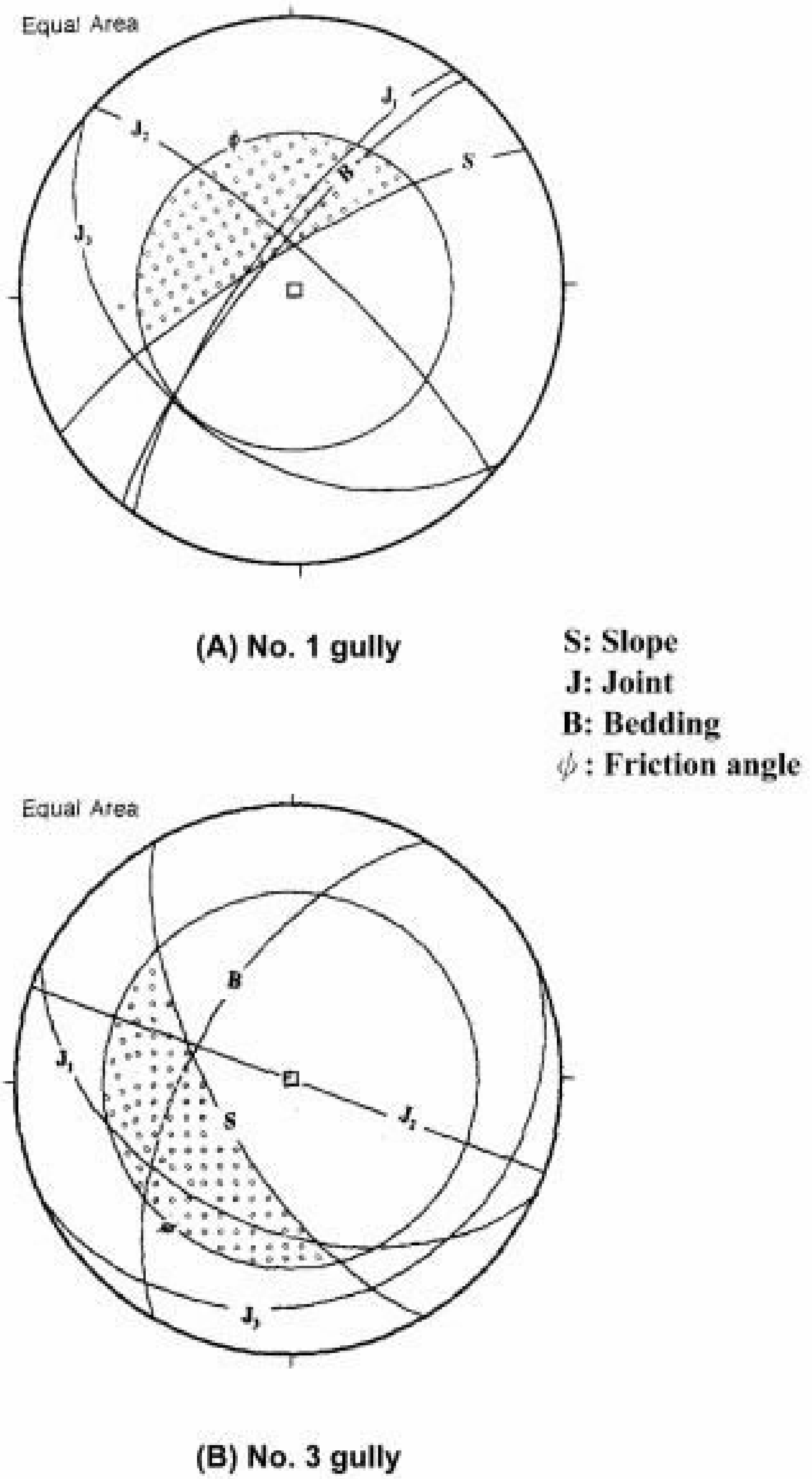

Fig. 2 Stereonet analysis of No.1 and No.3 gullies with dotted area showing the potential unstable areas.